

The Influence of Eddy Effect of Coils on Flow and Temperature Fields of Molten Droplet in Electromagnetic Levitation Device



LIN FENG and WAN-YUAN SHI

In this work, the influence of eddy effect of coils on magnetic, flow, and temperature fields in an electromagnetically levitated molten droplet was investigated by a series of axisymmetric numerical simulations. In an electromagnetic levitation device, both metal droplet and coils are conductive materials, therefore the distributions of current density in them should be non-uniform as a result of the eddy effect. However, in previous works, the eddy effect was considered alone in metal droplet but ignored in coils usually. As the distance of coils and metal droplet is several millimetres in general, the non-uniform distribution of current density in coils actually gives important influences on calculations of magnetic, flow, and temperature fields. Here, we consider the eddy effect both in metal droplet as well as that in coils simultaneously. Lifting force, absorbed power, fluid flow, and temperature field inside a 4-mm radius molten copper droplet as a typical example are then calculated and analyzed carefully under such condition. The results show that eddy effect leads to higher magnetic force, velocity, and temperature in both levitating and melting processes than those when the eddy effect is ignored. What is more, such influence increases as the distance of droplet and coils becomes closer, which corresponds to experimental measurement. Therefore, we suggest that eddy effect of coils should be considered in numerical simulation on this topic to obtain more reliable result.

DOI: 10.1007/s11663-015-0360-8

© The Minerals, Metals & Materials Society and ASM International 2015

I. INTRODUCTION

THE electromagnetic levitation (EML) is a widely used technique in material processing. Materials are levitated in space and avoid direct contacts with containers, which is of vital importance for the study of nucleation and the undercooled liquid metals. In addition, thermophysical properties of molten materials can also be measured by EML technique, such as surface tension, electrical conductivity, viscosity, and thermal conductivity.^[1-7] Since Muck^[8] first proposed the idea of electromagnetic levitation in 1923, several devices have been designed for positioning and melting materials, among which the TEMPUS unit developed by German scientists is well known for separately controlling levitation process and melting process. Very encouraging results have been gained through several Space Shuttle missions using the TEMPUS unit.

There are two sets of electromagnetic coils used for positioning and melting materials, respectively in electromagnetic levitation device. The first one operating at a relatively low load is positioning coils, which is used to levitate the materials. The second set of coils operates at

a higher load and provides energy to heat the materials. In this way, the heating and positioning processes are controlled independently.^[9] Upon that, the undercooling of metals can be realized when the heating coils are shut off.

In the EML technique, the magnetic force and absorbed power play an important role. With the holding of magnetic force, the sample could levitate in space and the absorbed power enables it to be heated and melted. Lifting force induced by high-frequency circle current was measured experimentally, but fits well with analytical results only when the sample is far away from coils.^[10] The analytical solution of absorbed power of the sample was given by Lohfer through solving the simplified Maxwell equations using Bessel functions.^[11] Calculations of lifting force and absorbed power in TEMPUS were carried out by Zong and Szekely using the volume integral method.^[12]

Beyond that, many works were focused on the fluid flow and the stability of the metal in levitation and melting process. Some simulations and experiments showed that the sample levitated in electromagnetic coils tends to be unstable. When the sample is melted, the electromagnetic force generated by coils together with buoyancy and Marangoni convection drive the internal flow of the sample and the velocity tends to be the value of 10 to 40 cm/s.^[13-19] The transition of laminar and turbulent flow was detected experimentally at a Reynolds number of 600.^[20] Applying an extra static magnetic field, the sample in electromagnetic levitation device appears to be more stable^[21-23] and

LIN FENG, Ph.D. Student, is with the College of Power Engineering, Chongqing University, Chongqing 400044, P. R. China. WAN-YUAN SHI, Professor, is with the College of Power Engineering, Chongqing University and also with the Key Laboratory of Low-grade Energy Utilization Technologies and Systems, Ministry of Education, Chongqing 400044, P. R. China. Contact e-mail: shiwy@cqu.edu.cn

Manuscript submitted December 13, 2014.

Article published online April 30, 2015.

Tsukada and coworkers^[24,25] suggested the measurement of thermal conductivity of molten Si can be implemented precisely when a static magnetic field of 4T is applied.

In most previous work, the calculations of magnetic field were usually based on an old algorithm of mutual inductance^[26] which derived the vector potential from Maxwell equations for simplification and considered current distribution in coils as a constant value. Thus, eddy effect of coils was ignored. In fact, considerable errors happen in this simplification and many works suggested that the calculation of magnetic field in high frequency should solve the vector potential and scalar potential simultaneously.^[26] In this paper, we calculate the original form of Maxwell equations in electromagnetic levitation device based on the finite element method (FEM) and present a comparison of considering and ignoring the eddy effect of coils, providing more accurate calculations of magnetic, flow, and temperature fields. In the following sections, the current arrangement in coils is discussed first and a quadrupole-heating model is adopted. The lifting force, absorbed power, velocity, and temperature field inside a molten copper droplet with radius of 4 mm are then calculated with and without eddy effect. The influences of eddy effect of coils on them are analyzed finally.

II. PHYSICAL MODEL

The configuration of TEMPUS unit is shown in Figure 1. For positioning coils, the current directions of the upper and lower coils are opposite, which produces a symmetrical magnetic field and holds the droplet firmly in the middle of the model. For heating coils, its function is to provide huge energy to melt the droplet. Theoretically, as long as a strong excitation is applied to heating coils, it can melt the droplet easily. However, positioning and heating are processes that happen simultaneously and heating should not affect the positioning process. In traditional TEMPUS, the two-frequency source is used and the heating coils operate at high frequency with low current amplitude, while positioning coils operate at low frequency with high current. Under this circumstance, the heating coils generate quite small magnetic force, thus heating process will not affect positioning process. However, the system of two-frequency source is much more complex than that of ordinary source and may lead to large temperature gradients as there is only one heating area on droplet. In this paper, it is replaced by a single-frequency model and the current arrangement of heating coils in it is rearranged correspondingly.

The current direction of heating coils can be arranged in three ways: (a) All the heating coils are of the same direction (adopted by traditional TEMPUS model). (b) The upper and lower coils are of opposite direction and opposite to positioning coils. (c) The upper and lower coils are of opposite direction and the same of positioning coils (named quadrupole-heating model hereafter, as seen in Figure 1). For the first kind of heating coils, the asymmetric current arrangement of heating coils can

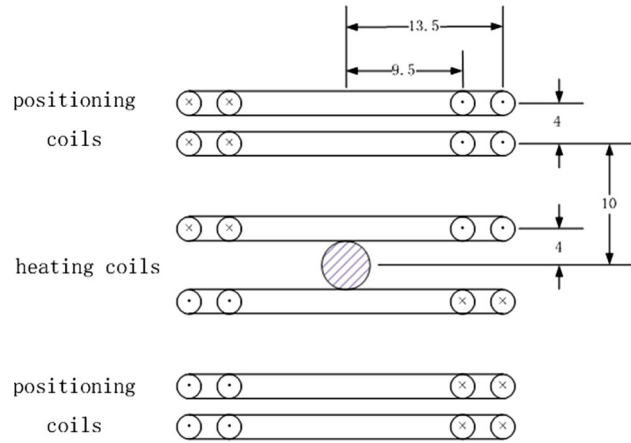


Fig. 1—Schematic diagram of electromagnetic levitation device.

hardly levitate the droplet steadily in single-frequency EML device. For the second kind of heating coil arrangement, the magnetic field will be self-canceled largely since the current direction in coils changes alternately. Hence, both the positioning process and heating process are of low efficiency. The third kind of heating coils combines the advantages of the two heating coils above, holding the droplet firmly and heating it efficiently. Consequently, the following calculations are based on the third case, *i.e.*, the quadrupole-heating model.

III. MATHEMATICAL MODEL

An axisymmetric model is adopted to calculate the magnetic and flow fields. The magnetic field is calculated first, and then Lorentz force and absorbed power are submitted into commercial software of Fluent to calculate the flow and temperature fields. For the metal droplet, a 4-mm radius copper sphere is used as an example to study the influences of eddy effect of coils in levitation process and melting process. Physical properties of molten copper and operating conditions are listed in Table I.

A. Electromagnetic Fields

Here, the system of electromagnetic levitation device is approximated as a magnetoquasistatic situation. The calculations of magnetic fields are under follow assumptions: (1) The shape of metal is a perfect sphere. (2) The model is axially symmetric. (3) Properties of metal are linear and isotropic. (4) There is no net charge in system. The time-harmonic Maxwell equations are expressed as:

$$\nabla \times \mathbf{H} = \mathbf{J} \quad [1]$$

$$\nabla \times \mathbf{E} = -j\omega\mathbf{B} \quad [2]$$

$$\mathbf{J} = \sigma\mathbf{E} \quad [3]$$

Table I. Physical Properties of Molten Copper and Processing Conditions in This Work

<i>Physical properties of molten copper</i>	
Viscosity (Pa s)	0.004
Density (kg/m ³)	8000
Thermal conductivity (W/m K)	166.1
Emissivity (–)	0.3
Specific heat (J/kg K)	31.38
Electric conductivity (S/m)	5.0 × 10 ⁶
Melting point (K)	1356
<i>Operating conditions</i>	
Current in heating coils (A)	385
Current in positioning coils (A)	143
Operating frequency (kHz)	144
Ambient temperature (K)	298
Conductivity of coils (S/m)	6.0 × 10 ⁷

$$\mathbf{B} = \mu\mathbf{H} \quad [4]$$

To solve the Maxwell equations, magnetic vector potential \mathbf{A} is introduced, which is expressed as:

$$\mathbf{B} = \nabla \times \mathbf{A} \quad [5]$$

By substituting the magnetic flux intensity \mathbf{B} into Eq. [2], the scalar potential ϕ is expressed as:

$$\mathbf{E} = -j\omega\mathbf{A} - \nabla\phi \quad [6]$$

Combined with Eq. [3], the current density \mathbf{J} is rewritten as the Eq. [7]:

$$\mathbf{J} = \mathbf{J}_e + \mathbf{J}_s = -\sigma j\omega\mathbf{A} - \sigma\nabla\phi, \quad [7]$$

where \mathbf{J}_s represents the source current density due to differences in electric potential, and \mathbf{J}_e represents the induced eddy current density due to time-varying magnetic fields. For stranded conductors, the current density $\mathbf{J} = \mathbf{J}_s$ and eddy current density is neglected. For solid conductors, $\mathbf{J} = \mathbf{J}_e + \mathbf{J}_s$.

The total current flow of \mathbf{I} in conductor can be expressed as:

$$\mathbf{I} = \int_{\Omega} \mathbf{J} d\Omega = \int_{\Omega} (-\sigma j\omega\mathbf{A} - \sigma\nabla\phi) d\Omega \quad [8]$$

This is the first equation for solving the vector potential and scalar potential in magnetic field. The second equation could be obtained through Eqs. [1], [4], [5], and [7]:

$$\nabla \times 1/\mu(\nabla \times \mathbf{A}) = -\sigma j\omega\mathbf{A} - \sigma\nabla\phi \quad [9]$$

Equations [8] and [9] show that the vector potential and scalar potential are coupled with each other. As a result, these two variables should be solved simultaneously and all the properties in magnetic field could be expressed as a function of them. Assuming that the current density \mathbf{J} and vector potential \mathbf{A} are constant in longitudinal direction, Eq. [9] is rewritten as:

$$(\nabla \cdot 1/\mu\nabla)\mathbf{A} - \sigma j\omega\mathbf{A} - \sigma\nabla\phi = 0 \quad [10]$$

By solving Eqs. [7] and [10], the vector potential \mathbf{A} is obtained. Then the current density \mathbf{J} and magnetic flux intensity \mathbf{B} can be solved. The time-averaged Lorentz force and power absorption on objects are given by

$$\mathbf{F} = 0.5\text{Re}(\mathbf{J} \times \mathbf{B}^*) \quad [11]$$

$$\Phi_v = 0.5\text{Re}(\mathbf{J} \cdot \mathbf{J}^*/\sigma), \quad [12]$$

where the symbol of Re represents the real part of a complex quantity and asterisk designates the complex conjugate. The lifting force is calculated from the vertical component of magnetic force of \mathbf{F} .

B. Flow and Temperature Fields

Flow inside the molten droplet is assumed to be incompressibly laminar. The governing equations include the continuity equation, Navier–Stokes equations and energy conservation equations.

$$\nabla \cdot \mathbf{u} = 0 \quad [13]$$

$$\frac{\partial \mathbf{u}}{\partial t} + (\mathbf{u} \cdot \nabla)\mathbf{u} = -\frac{1}{\rho}\nabla p + \nu\nabla^2\mathbf{u} + \frac{1}{\rho}\mathbf{F} \quad [14]$$

$$\rho c_p \left(\frac{\partial T}{\partial t} + \mathbf{u} \cdot \nabla T \right) = \lambda\nabla^2 T + \Phi_v \quad [15]$$

The boundary conditions are as follows. At the droplet surface:

$$\mathbf{u} \cdot \mathbf{n} = 0 \quad [16]$$

$$-\lambda\nabla T \cdot \mathbf{n} = \varepsilon\sigma_{\text{sb}}(T^4 - T_a^4) \quad [17]$$

At the centerline:

$$\mathbf{u} \cdot \mathbf{n} = \nabla T \cdot \mathbf{n} = 0 \quad [18]$$

Obviously, the surface tension is not considered because the droplet is assumed to be a fixed perfect sphere. Marangoni effect is also ignored because previous work showed that the Lorentz force is several orders of magnitude larger than that of Marangoni force.^[27] The flow inside molten droplet driven by Lorentz force tends to form the two anti-rotating recirculating loops. In reality, it is flow between laminar regime and turbulent regime, and the viscosity is enhanced by the order of 10 to 40.^[15] So far, there is no adequate flow model for such kind of weak turbulent flows. Referring from Li *et al.*,^[15] the fluid flow is assumed to be laminar but the viscosity is artificially enlarged on the orders of 10 to compensate the differences. They obtained satisfying results and we thus adopted such method in the following calculations.

IV. RESULTS AND DISCUSSION

A. Magnetic Field

To confirm the validity of our calculation, a comparison of our results of lifting force and absorbed power by positioning coils with those in Reference 13 is carried out, as shown in Figure 2. Lifting forces marked by circles are data ignoring the eddy effect of coils, and marked by plus sign are our results considering the eddy effect. The maximum error between them is 5.0 pct. When comparing with experimental results, the error is reduced to be 3.75 pct. Our results show better consistency than that of ignored eddy effect. Due to lack of experimental data for absorbed power in opening references according to our knowledge, here we only compare our numerical result with those analytical results by Lohfer.^[11] In his analysis, he took the eddy current in coils as a constant number. In order to compare with his result, we also ignored the eddy effect of coils and regarded it as constant number. The maximum error is 2.2 pct. Our result is good agreement with his result. These comparisons confirm that our calculations are valid and reliable.

Figure 3 exhibits the distribution of magnetic field intensity of droplet and the time-averaged magnetic force in levitating process (Figure 3(a)) and melting process (Figure 3(b)). It can be seen that both the magnetic field intensity and magnetic force in melting process are much stronger than that in levitating process. However, the patterns of the two fields in heating process are different from that in Reference 12 which is due to differences of heating coil arrangement.

In both positioning and melting process, eddy effect enables the current distribution in coils to be non-uniform, as shown in Figure 4. For the upper part the eddy effect is considered but the lower part ignored. Great differences can be seen even if all the coils are of the same excitation, indicating the important influences of eddy effect. When the eddy effect is considered, the current densities of inner areas of coils are much larger than those of other areas, which will definitely influence the further calculations of magnetic, flow, and temperature fields.

In the positioning process, when the eddy effect is considered both the lifting force and absorbed power are larger than those without eddy effect, as shown in Figure 5. Such difference increases when the metal drifts upper or lower, because the distance of coils and droplet becomes closer in this occasion and the impact of eddy effect becomes stronger (seen in Section IV-B). The average relative error of lifting force and absorbed power are 10.5 and 16.5 pct, respectively, which is considerable.

In the heating process, similar difference with error of 10.5 pct can be seen for absorbed power (Figure 6). However, the difference of lifting force reduces to a relative low level with error of 1.65 pct. We notice that the distance of heating coils and droplet is very close in this occasion (Figure 1). When eddy effect of coils is considered, the angle between magnetic force vector and horizontal plane decreases, causing the decrease of

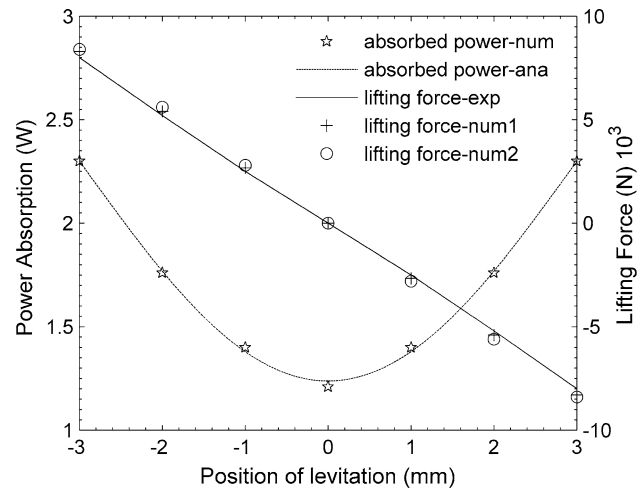


Fig. 2—Calculated lifting force and absorbed power in levitating process vs those results in Ref. [13].

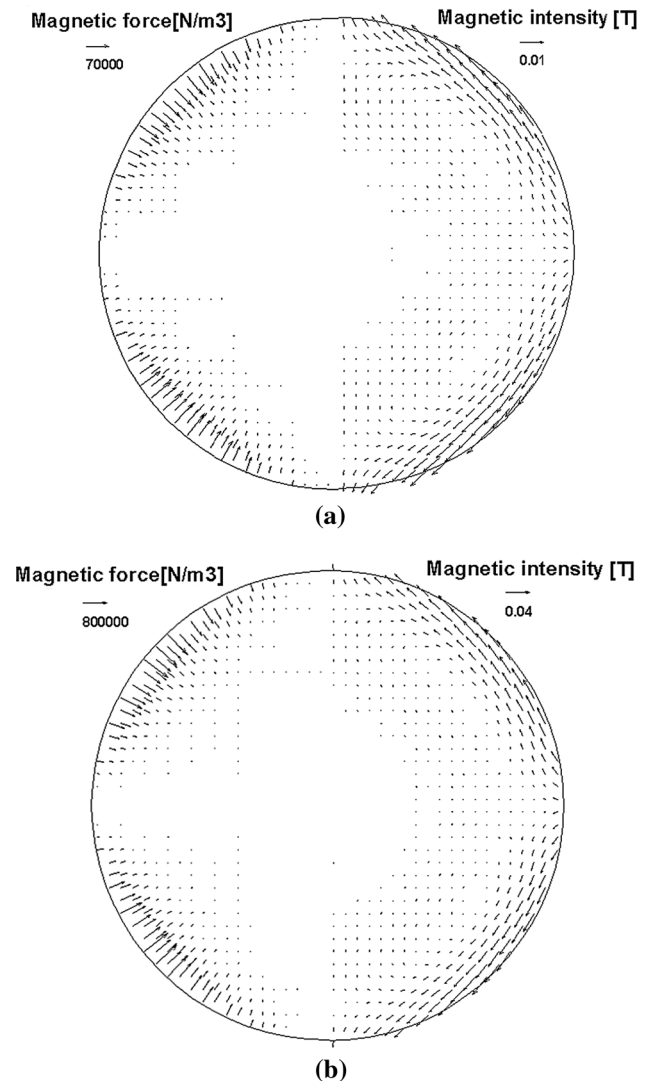


Fig. 3—Magnetic field and magnetic force in droplet generated by positioning coils (a) and positioning and heating coils (b).

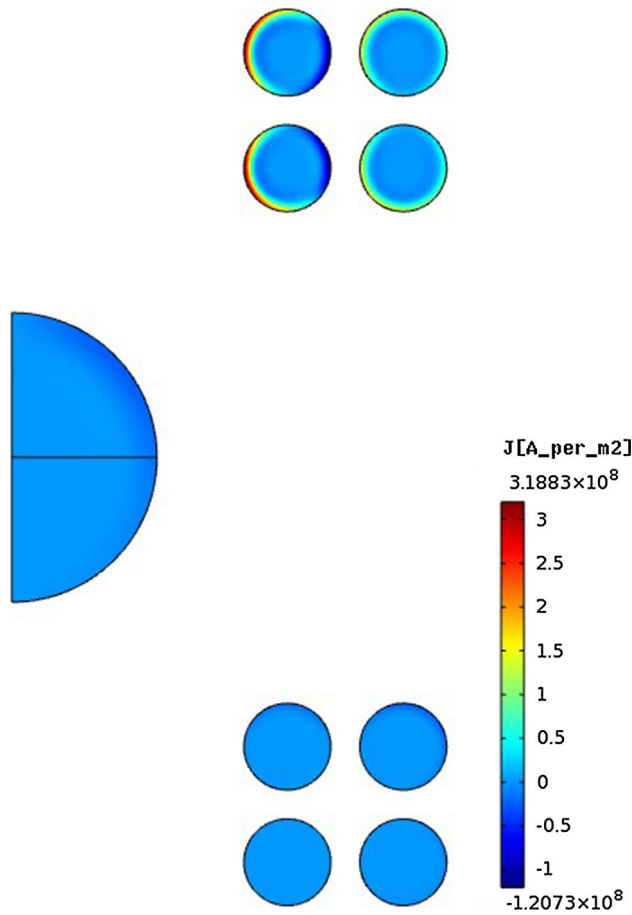


Fig. 4—Current distribution in coils considering (upper) and ignoring (lower) the eddy effect.

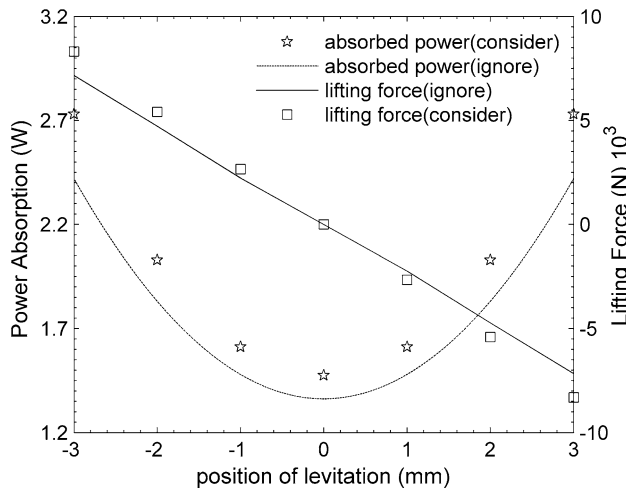


Fig. 5—Power absorption and lifting force in levitating process with and without eddy effect.

lifting force. Thus influence of eddy effect on lifting force is minished and lifting force is not suitable to measure the influence of eddy effect in this situation. However, the absorbed power is a scalar variable, which can be used to measure the influences of eddy effect.

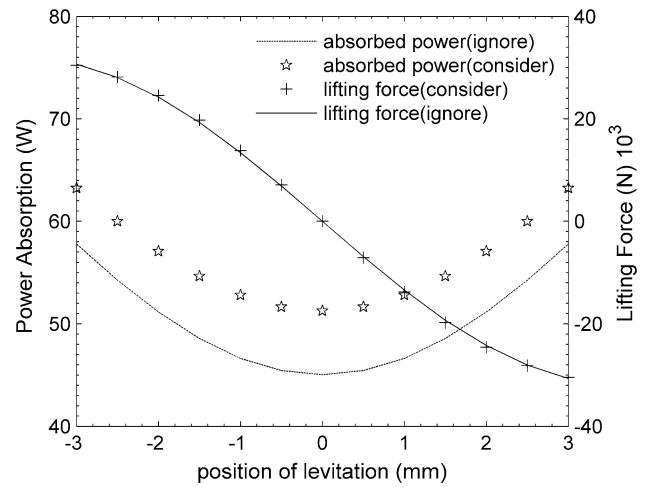


Fig. 6—Lifting force and absorbed power in melting process considering vs ignoring eddy effect.

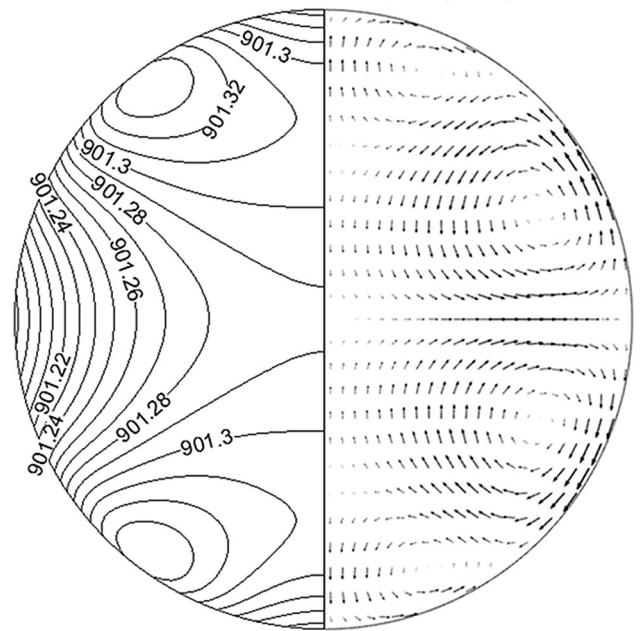
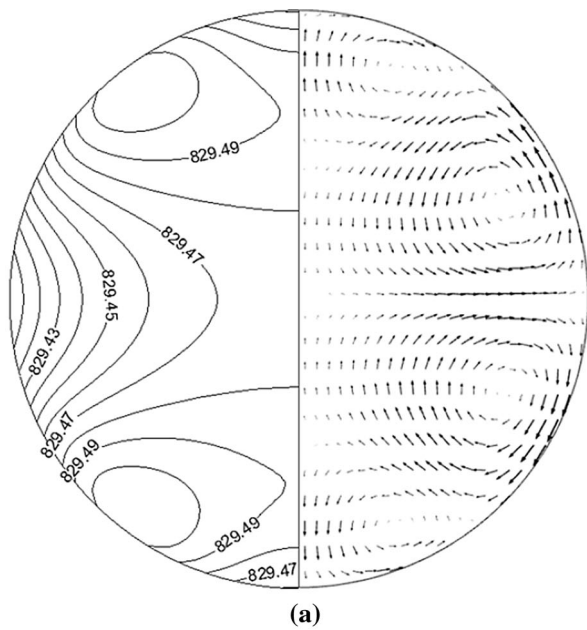


Fig. 7—Flow field (right) and isotherm counters (left) inside a 5-mm radius silver droplet in levitating process.

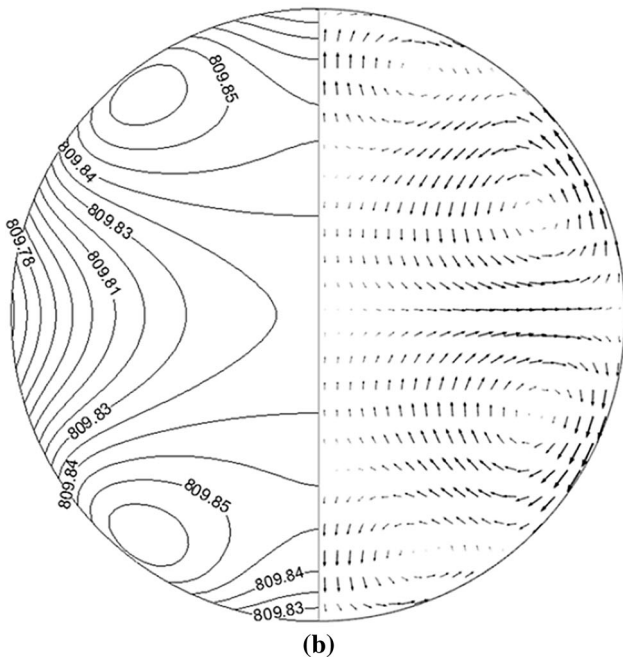
B. Fluid Flow and Temperature Fields

Flow and temperature fields are also verified through comparing with the results from Li and Song^[15] and rather good consistence indicates that our simulation results are reliable, as seen in Figure 7. There are two vortices induced by electromagnetic force for each quarter of the droplet, which were observed in many works.^[15,16,23–26] The isotherm lines of ours and those in Reference 15 are very familiar, with a relative error of less than 0.5 pct. The maximum velocity by our calculation is 4.47 cm/s, very close to that of 4.39 cm/s.

As mentioned above, the current density distribution in coils influences the calculations of magnetic force and absorbed power. Undoubtedly, the flow field and



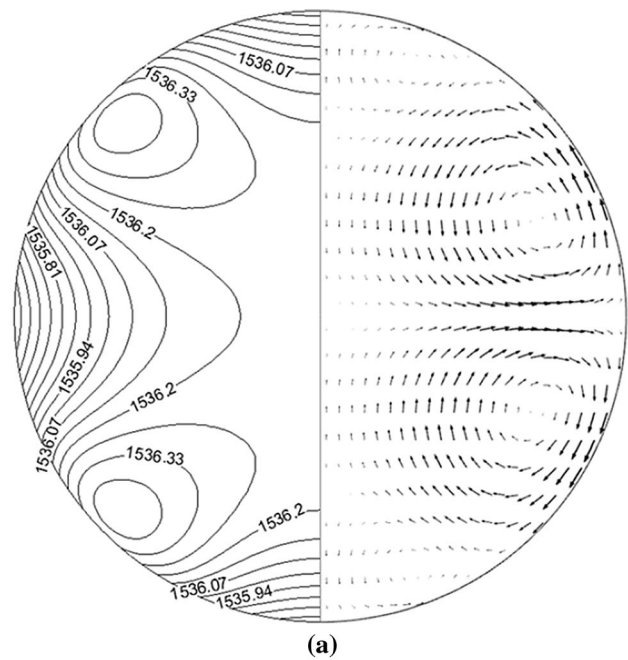
(a)



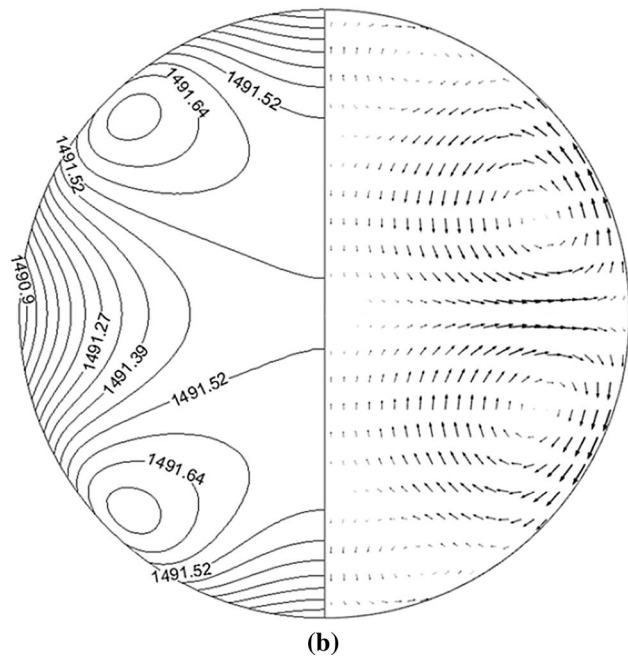
(b)

Fig. 8—Temperature and flow fields considering eddy effect (a) and ignoring eddy effect (b) in levitating process.

temperature field will be affected because both of them are induced by magnetic force and absorbed power. Figure 8 shows such an example for positioning process. Although the temperature field and flow field of the two cases are quite similar, the maximum velocity considering eddy effect is 3.04 cm/s while 2.76 cm/s when eddy effect is ignored with relative error is 10.1 pct. The difference of maximum temperature is 20 K with relative error of 2.4 pct, which is much smaller than velocity. The reason is that the radiation of heat becomes larger with the increasing of temperature. Thus the temperature difference is minished, however, with an error of 20 K still.



(a)



(b)

Fig. 9—Temperature and flow fields considering eddy effect (a) and ignoring eddy effect (b) in melting process.

When heating coils are introduced, higher excitation induces stronger convection and higher temperature inside the molten droplet, as shown in Figure 9. Consequently, the influence of eddy effect becomes more significant. The maximum velocity with eddy effect is 30.64 cm/s but it is 27.6 cm/s without eddy effect. The difference of maximum temperature between two cases rises up to 45 K, which is quite larger than that in Figure 8. Moreover, we believe that the closer distance between the droplet and heating coils is another reason causing the increasing influence of eddy effect.

As mentioned above, the distance of droplet and coils is an important factor when eddy effect is considered. For instance, for a 5-mm radius copper droplet, the velocity and temperature differences are 5.81 cm/s and 59 K, respectively, which are rather larger than those of 4 mm radius. In practical applications, the distance of coils and metal is even closer to obtain stronger magnetic field and the differences will be larger. Actually, Yun *et al.*^[10] found that the lifting force in experiment fits well with analytical curves when the distance is relatively large while badly when the distance is small. Thus, it is essential to consider the eddy effect of coils in numerical simulations to obtain more reliable result.

V. CONCLUSIONS

In this work, to investigate the influence of eddy effect of coils on EML-levitated metal droplet, the magnetic, flow, and temperature fields of copper droplet with radius of 4 mm are calculated. The results show that eddy effect tends to generate a larger magnetic field, then flow and temperature fields are influenced too. A relative error of over 10 pct is seen in maximum velocity in both levitating and melting processes if eddy effect is neglected. The temperature level is 20 K higher in levitating process while 45 K higher in melting process when eddy effect is considered. The differences become even larger when the distance between coils and metal is closer. Hence the bigger the metal is, the more apparent the influence of eddy effect will be. We suggest that the eddy effect of coils should be considered in numerical simulation to obtain more reliable result.

ACKNOWLEDGMENTS

This work was supported by National Natural Science Foundation of China (Grant No. 51176210), Natural Science Foundation Project of CQ cstc2012jjA5003.

LIST OF SYMBOLS

A	Magnetic vector potential (–)
B	Magnetic flux intensity (T)
c_p	Specific heat (J/kg K)
E	Electric field vector (V/m)
F	Lorentz force (N/m ³)
H	Magnetic field intensity (A/m)
I	Total current (A)
j	$=\sqrt{-1}$
J	Current density vector (A/m ²)
J_e	Induced eddy current density (A/m ²)
J_s	Source current density (A/m ²)
T	Temperature (K)
T_a	Ambient temperature (K)

u	Velocity vector (m/s)
ε	Emissivity (–)
ϕ	Scalar potential (–)
Φ_V	Power absorption (W/m ³)
λ	Thermal conductivity (W/m K)
μ	Magnetic permeability (H/m)
ρ	Density (kg/m ³)
σ	Electric conductivity (S/m)
σ_{sb}	Stefan–Boltzmann constant (W/m ² K ⁴)
τ	Period of current (s)
ν	Kinematic viscosity (m ² /s)
ω	Frequency of current (Hz)
Ω	Cross-sectional area of the conductor

REFERENCES

1. W.K. Rhim, S.K. Chung, D. Barber, K.F. Man, G. Gutt, A. Rulison, and R.E. Spjut: *J. Rev. Sci. Instrum.*, 1993, vol. 64, pp. 2961–70.
2. J. Brillo, I. Egly, H.S. Giffard, and A. Patti: *Int. J. Thermophys.*, 2004, vol. 25, pp. 1881–88.
3. M.B. Robinson, R.J. Bayuzick, and W.H. Hofmeister: *Adv. Space Res.*, 1988, vol. 8, pp. 321–30.
4. D.M. Herlach: *Annu. Rev. Mater. Sci.*, 1991, vol. 21, pp. 23–44.
5. S. Sauerland, K. Eckler, and I. Egly: *Thermochim. Acta*, 1993, vol. 218, pp. 445–53.
6. I. Egly, G. Lohofer, I. Seyhan, S. Schneider, and B. Feuerbacher: *Int. J. Thermophys.*, 1999, vol. 20, pp. 1005–15.
7. Y. Inatomi, F. Onishi, K. Nagashio, and K. Kuribayashi: *Int. J. Thermophys.*, 2007, vol. 28, pp. 44–59.
8. O. Muck: German Patent, No. 422004, 1923.
9. J.H. Zong, J. Szekely, and E. Schwart: *IEEE T Magn.*, 1992, vol. 28, pp. 1833–42.
10. Y. Yun, X. Tai, G. Li, and W. Zhang: *Physics Experimentation*, 2002, vol. 22, pp. 9–11 (In Chinese).
11. G. Lohfer: *Siam J. Appl. Math.*, 1989, vol. 49, pp. 567–81.
12. J.H. Zong and J. Szekely: *Acta Astronaut.*, 1993, vol. 29, pp. 371–78.
13. J.H. Zong, L. Benqiang, and J. Szekely: *Acta Astronaut.*, 1992, vol. 26, pp. 435–49.
14. J.H. Zong, L. Benqiang, and J. Szekely: *Acta Astronaut.*, 1993, vol. 29, pp. 305–311.
15. B.Q. Li and S.P. Song: *Microgravity Sci. Technol.*, 1998, vol. 11, pp. 134–43.
16. R.W. Hyers: *Meas. Sci. Technol.*, 2005, vol. 16, pp. 394–401.
17. V. Bojarevics and K. Pericleous: *ISIJ Int.*, 2003, vol. 43, pp. 890–98.
18. J. Lee, D.M. Matson, S. Binder, M. Kolbe, D. Herlach, and R.W. Hyers: *Metall. Mater. Trans. B*, 2014, vol. 45B, pp. 1018–23.
19. J. Lee, X. Xiao, D.M. Matson, and R.W. Hyers: *Metall. Mater. Trans. B*, 2014, vol. 46B, pp. 199–207.
20. R.W. Hyers, G. Trapaga, and B. Abedian: *Metall. Mater. Trans. B*, 2003, vol. 34B, pp. 29–36.
21. S. Ozawa, T. Koda, M. Adachi, K. Morohoshi, M. Watanabe, and T. Hibiya: *J. Appl. Phys.*, 2009, vol. 106, p. 034907-1-7.
22. H. Yasuda, I. Ohnaka, Y. Ninomiya, R. Ishii, S. Fujit, and K. Kishio: *J. Cryst. Growth.*, 2004, vol. 260, pp. 475–85.
23. K. Pericleous, V. Bojarevics, and A. Roy: *IJMSA*, 2013, vol. 30, pp. 56–63.
24. T. Tsukada, K.-I. Sugioka, T. Tsutsumino, H. Fukuyama, and H. Kobatake: *Int. J. Heat Mass Trans.*, 2009, vol. 52, pp. 5152–57.
25. K. Sugioka, T. Tsukada, H. Fukuyama, H. Kobatake, and S. Awaji: *Int. J. Heat Mass Trans.*, 2010, vol. 53, pp. 4228–32.
26. R.F. Dudley and P. Burke: *IEEE Trans. Ind. Appl.*, 1972, vol. 8, pp. 565–71.
27. B.Q. Li and S.P. Song: *J. Heat Transfer*, 1998, vol. 120, pp. 492–504.